

# Control Model of a Small Micro-class UAV Object Taking Into Account the Impact of Strong Wind

LUCJAN SETLAK, RAFAŁ KOWALIK  
Department of Avionics and Control Systems  
Polish Air Force University  
ul. Dywizjonu 303 nr 35, 08-521 Deblin  
POLAND

l.setlak@law.mil.pl, r.kowalik@law.mil.pl, <http://www.law.mil.pl/index.php/pl/>

*Abstract:* - The subject of this article is to analyze and select simulation tests in the field of issues related to flight control systems for micro-class aircraft. The main purpose of the work is to develop an algorithm for the flight control system, taking into account both the speed and direction of the wind acting on the UAV, which are the key attributes that play a decisive impact on the disturbance of flight parameters and its correct performance. What is more, atmospheric conditions determined by the influence of wind can produce phenomena dangerous to aviation in the form of wind shear or blast from the back during the landing process of the aircraft. The occurrence of the above situation may be the cause of stall phenomenon, which in turn may be the cause of a dangerous aviation phenomenon (accident, incident, etc.). For the purposes of solving the research problem, the article uses a mathematical apparatus in the form of equations describing the movement of the aircraft and the forces and moments acting on it. Based on the mathematical analysis of the UAV object, in the further part of the article, an algorithm was developed to estimate the impact of wind and an analysis of measurement errors occurring during flights and their impact on the measured values, as well as the values calculated on their basis. On this basis, charts have been developed defining clearly the various relationships. In the final part of the thesis, based on the mathematical analysis, simulation tests and analysis of the results obtained, the final conclusions and observations were formulated, which are reflected in practical applications.

*Key-Words:* - Control model, micro class UAV object, equations of motion, strong wind influence

## 1 Introduction

According to the authors of this work, modern flying objects, including unmanned aerial vehicles, are not a homogeneous group, which should be particularly considered in relation to reconnaissance, inspection and transport applications [1], [2].

The article compares the different types of aircraft, and the source of knowledge is a critical analysis of the literature on the subject of research and experience gained while designing, performing flights on own unmanned vehicles and during participation in numerous professions related to inspection, rescue and transport tasks, e.g. Droniada, ERL (*European Robotics League*) Emergency Robots, etc. The experience gained resulted in the creation of guidelines for the proprietary unmanned aerial vehicle V/STOL (*Vertical/Short Take Off and Landing*), which can be used in transport missions and flight inspection [3], [4], [5].

It should be noted that powered rotorcraft, i.e. multi-rotors are easy to fly, however they have significant disadvantages associated with limited load capacity, speed and time of unattended operation.

In turn, very important of their features are both the possibilities of vertical take-off and landing, so they can be used in the implementation of transport tasks, as well as hovering capabilities useful when performing inspection tasks. Another key disadvantage of these vehicles is the high power demand associated with the lack of bearing surfaces, and the only source of lift are propellers driven by engines. It should also be noted that not only the drive unit is responsible for the entire load capacity, but for the purposes of flight stabilization, the drives constantly change their rotational speed, which in turn leads to significant energy losses [6], [7].

Although losses can be partly compensated for by using propellers with a larger diameter, however, using this technical approach, this type of solution simultaneously increases the inertia of the power unit. In addition, this inconvenience also affects the maximum capacity and the real inability to land safely in the event of a failure of the propulsion system or damage to batteries or lack of fuel.

Therefore, for a multi-rotor flight to be possible, it must be equipped with a flight controller that can stabilize the vehicle in the air, e.g. by applying

coordination of the functionality of all drives, which is impossible for a human. In addition, it should be remembered that thanks to the use of the achievements of modern electronics and MEMS (*Micro Electro Mechanical Systems*) microsystem sensors, flights of this type of aircraft are possible. [8], [9], [10].

In the case of airplanes or helicopters sufficiently stable, this type of controller is not required for the remote control task, but it should be noted that it will be necessary for autonomous flights. Based on the above redundancy that a multi-rotor can provide, it depends on the number of engines and their arrangement. In the case of a system with three or four rotors, damage to one propulsion means that this type of vehicle will not be able to stay in the air. However, if the same situation happens in a six-rotor system, as our experience shows, flight and safe landing will still be possible. Attention should also be paid to the high safety of multirotors in the X8 system. It is a drone system with four arms, at the ends of which there are two motors working in opposite directions.

This system ensures very good stability and is very resistant to loss of drive. If one of the engines is damaged, the vehicle does not lose its fulcrum. The advantage of this type of solution is also a simplified design (it has only four arms) and relatively small dimensions, compared to a multi-rotor equipped with eight drives on eight independent arms [11], [12].

A similar redundancy was observed for the Y6 system compared to the hexacopter system, however, taking into account the mechanical design of the multi-rotor, it is extremely simple. Typically, the construction of this type of vehicle involves the creation of a central attachment or a plate (*centerplate*) to which all arms (usually 3 to 6), the chassis and the rest of the required electronics and systems are attached. This simplicity means that the vehicles can be easily modified for various types of tasks. An excellent example is the design of a mobile laboratory, in which the vehicle not only transports the device, but after a simple modification forms part of it [13], [14]. Multirotors control is based on the synchronized thrust regulation of each drive, for which the flight controller is responsible. Sophisticated control systems make this type of structure extremely stable and easy to pilot, and additionally, using the GPS (*Global Positioning System*) system, they are able to extremely accurately autonomously maintain their position even in strong winds, which is the subject of research in this article [15].

## 2 Equations of motion

### 2.1 Aircraft flight rules

Complex aircraft equations include changes in flight specifications, e.g. aircraft mass, moving part dynamics, and design flexibility. For the purposes of this study, the presented equations with a significant degree of complexity have been simplified by assuming that the aircraft is a rigid body with a stable mass (no fuel consumption), the gravitational force is constant and the Earth reference system has been adopted as the main one. In addition, the *XOZ* plane in the structural system is a plane of symmetry, which is illustrated in the figure below (Fig. 1).

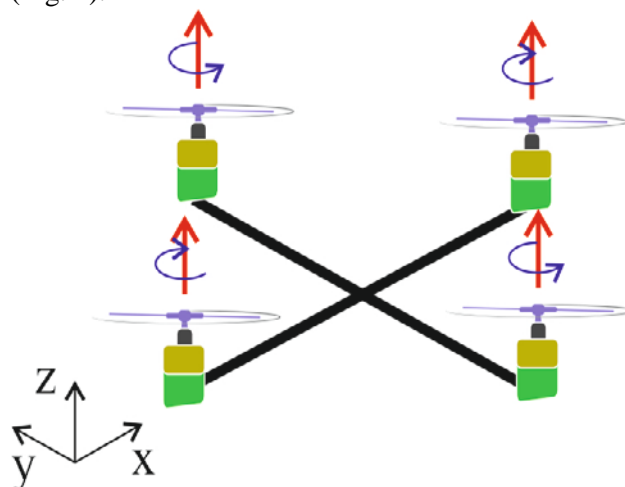


Fig. 1 Coordinate system for unmanned aerial vehicle

It should be noted that the derivation of all equations of motion is found in various literature, for example [16], [17], and the work uses only relevant for its purposes derived forms.

### 2.2 Equations of forces

Basic aircraft motion can be expressed using *Newton's* second law of dynamics (1):

$$\bar{F} = \bar{M}a_c = m \frac{d}{dt}(\bar{V}) \quad (1)$$

where  $\bar{F} = [F_x F_y F_z]^T$  - is force,  $a_c$  - acceleration of the aircraft's center of gravity,  $\bar{V} = [u v w]^T$  - flight speed vector,  $\bar{M} = [M_x M_y M_z]^T$  - moment acting on the aircraft,  $\omega = [p q r]^T$  - rotational speed vector, while  $I$  - internal matrix of the aircraft.

It should be noted that this rule only works for the center of gravity of the aircraft, moreover, these equations must be transformed into a reference system associated with the aircraft structure, according to equation below (2).

$$F_B = T_{BI}F = m \frac{d}{dt}(V_B) + m(\Omega_B)V_B \quad (2)$$

After substituting the relevant dependencies, 3 final equations of motion in the structural reference system (3) - (5) were obtained [18], [19]:

$$\dot{u} = \frac{1}{m}(X + T \cos(e_T)) - g \sin \theta + rv - qw \quad (3)$$

$$\dot{v} = \frac{1}{m}(Y) + g \sin(\varphi) \cos(\theta) + pw - ru \quad (4)$$

$$\dot{w} = \frac{1}{m}(Z + T \sin(e_T)) + g \cos \varphi \cos \theta + qu - pv \quad (5)$$

where:  $V_B = [u \ v \ w]^T$  - aircraft speed  $\dot{V}_B = [\dot{u} \ \dot{v} \ \dot{w}]^T$  - acceleration in the structural system,  $(F_A)_B = [X \ Y \ Z]^T$  - aerodynamic force vector,  $\omega_B = [p \ q \ r]^T$  - angular velocity,  $T_B = [T \cos e_T \ 0 \ T \sin e_T]^T$  - thrust vector, and  $e_T$  - is the thrust angle, usually takes zero value to simplify motion equations.

### 2.3 Equations of moments

From the equation (6) after transformation to the structural reference system, using the transformation matrix  $T_{BI}$  derived previously (earlier) and after applying additional operations, finally used equations of moments (6) - (7) were obtained [20], [21].

$$M = \frac{d}{dt} h \quad (6)$$

$$M_B = I_B \dot{\omega}_B + \Omega_B I_B \omega_B \quad (7)$$

Then, assuming that  $XOZ$  is a plane of symmetry, the elements in the internal matrix were zeroed, which was derived in equations (8) - (9).

$$I_B = \begin{bmatrix} I_{xx} & -I_{xy} & -I_{xz} \\ -I_{xy} & I_{yy} & -I_{yz} \\ -I_{xz} & -I_{yz} & I_{zz} \end{bmatrix} \quad (8)$$

$$I'_B = \begin{bmatrix} I_{xx} & 0 & -I_{xz} \\ 0 & I_{yy} & 0 \\ -I_{xz} & 0 & I_{zz} \end{bmatrix} \quad (9)$$

$$\dot{p} = \frac{I_{xx}}{I_D} [L + I_{xz}pq - (I_{zz} - I_{yy})qr] + \frac{I_{xz}}{I_D} [N - I_{xz}qr - (I_{yy} - I_{xx})pq] \quad (10)$$

$$\dot{q} = \frac{1}{I_{yy}} [M + M_T - (I_{xx} - I_{zz})pr - I_{xz}(p^2 - r^2)] \quad (11)$$

$$\dot{r} = \frac{I_{xz}}{I_D} [L + I_{xz}pq - (I_{zz} - I_{yy})qr] + \frac{I_{xx}}{I_D} [N - I_{xz}qr - (I_{yy} - I_{xx})pq] \quad (12)$$

After performing subsequent operations, the resulting equations of moments acting on the aircraft were obtained. The meaning of individual terms is as follows:  $M_B = [L \ M + M_T \ N]^T$  it is a moment vector and  $I_D = I_{xx}I_{zz} - I_{xz}^2$ .

$$I''_B = \begin{bmatrix} I_{xx} & 0 & 0 \\ 0 & I_{yy} & 0 \\ 0 & 0 & I_{zz} \end{bmatrix} \quad (13)$$

Some cases can be expressed in the main axes, as shown in the example of equation (13), so the equations of moments simplify to (14) - (16) [22]:

$$\dot{p} = \frac{L - (I_{zp} - I_{yp})qr}{I_{xp}} \quad (14)$$

$$\dot{q} = \frac{M + M_T - (I_{xp} - I_{zp})pr}{I_{yp}} \quad (15)$$

$$\dot{r} = \frac{N - (I_{yp} - I_{xp})pq}{I_{zp}} \quad (16)$$

### 2.4 Equations of motion

It was necessary to use aircraft motion equations. In this subsection they have been presented with reference to the structural system and expressed in the following form (17) - (19):

$$\dot{\varphi} = p + (q \sin \varphi + r \cos \varphi) \tan \theta \quad (17)$$

$$\dot{\theta} = q \cos \varphi - r \sin \varphi \quad (18)$$

$$\dot{\psi} = (q \sin \varphi + r \cos \varphi) \sin((\sec) \theta) \quad (19)$$

## 2.5 Equations of navigation

The next important step was the presentation of navigation equations. In this subsection they are given in relation to the structural system and expressed in the following form (20) - (23):

$$\begin{bmatrix} \dot{x}_E \\ \dot{y}_E \\ \dot{z}_E \end{bmatrix} = T_{IB} \begin{bmatrix} u \\ v \\ w \end{bmatrix} \quad (20)$$

$$\begin{aligned} \dot{x}_E = & u(\cos \theta \cos \psi) \\ & + v(\sin \varphi \sin \theta \cos \psi \\ & - \cos \varphi \sin \psi) \\ & + w(\cos \varphi \sin \theta \cos \psi \\ & + \sin \varphi \sin \psi) \end{aligned} \quad (21)$$

$$\begin{aligned} \dot{y}_E = & u(\cos \theta \sin \psi) \\ & + v(\sin \varphi \sin \theta \sin \psi \\ & + \cos \varphi \cos \psi) \\ & + w(\cos \varphi \sin \theta \sin \psi \\ & - \sin \varphi \cos \psi) \end{aligned} \quad (22)$$

$$\dot{h} = -\dot{z}_E = u \sin \theta - v \sin \varphi \cos \theta - w \cos \varphi \cos \theta \quad (23)$$

## 3 Flight control algorithm of unmanned aerial vehicle in the presence of a strong wind

In a special situation, when the aircraft is not moving and the surrounding atmosphere flows in a direction parallel to the  $X$  axis of the structural system (as in the case of wind tunnels), it can be assumed that the speed of the aircraft relative to the surrounding air masses is equal to the flow velocity of the atmosphere.

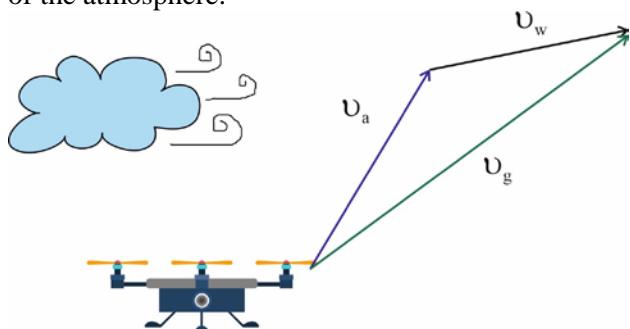


Fig. 2 A vector triangle of the wind

When considering some wind disturbances in the atmosphere, the wind vector should be added to the atmosphere velocity vector. The resulting vector is the speed of the aircraft relative to the surrounding air masses. Applying this principle on a flying aircraft, the relationship is obtained that the speed of

the aircraft relative to the atmosphere minus the wind speed relative to the Earth is the speed of the aircraft relative to the Earth (traveling speed) [23], [24].

This situation is shown in Figure 2 and in equation (24), where:  $V_g$  - traveling speed of the aircraft,  $V_a$  - speed in the aerodynamic system (relative to the surrounding air masses), and  $V_w$  - wind speed in the Earth-related system.

$$V_g = V_a + V_w \quad (24)$$

After expressing the wind speed components from equation (24), equations (25), (26), (27) are obtained: where:  $\alpha$  - angle of attack,  $\beta$  - angle of slide,  $\gamma = \theta - \alpha$  - angle of flight path,  $\psi$  - course,  $[\dot{x} \ \dot{y} \ \dot{z}]^T$  - traveling speed of the aircraft,  $V_a$  - speed in relation to the structural system.

For the following equations, it is assumed that the tilt angle  $\varphi$  is equal to 0 [25], [26].

$$V_{wx} = \dot{x} - V_a \cos \gamma \cos \beta \cos \psi + V_a \cos \gamma \sin \beta \sin \psi \quad (25)$$

$$V_{wy} = \dot{y} - V_a \cos \gamma \cos \beta \sin \psi - V_a \cos \gamma \sin \beta \cos \psi \quad (26)$$

$$V_{wz} = \dot{z} - V_a \sin \gamma \quad (27)$$

For the algorithm taking into account wind, the general form of calculation equations is needed, thanks to which it will be possible to calculate wind speed during aircraft maneuvers such as correct bend, using a controlled angle of tilt.

To do this, express the speed of the aircraft relative to the surrounding air masses in the Earth-related reference system using the transformation matrix  $R_I^B$  and  $R_B^W$  obtained in subsection 2.2.

The final, extended equations of the wind estimation algorithm were derived as follows, according to the following form (28):

$$\begin{bmatrix} V_{wx} \\ V_{wy} \\ V_{wz} \end{bmatrix} = \begin{bmatrix} \dot{x} \\ \dot{y} \\ \dot{z} \end{bmatrix}_{GPS} - R_I^B R_B^W \begin{bmatrix} V_a \\ 0 \\ 0 \end{bmatrix} \quad (28)$$

It should be noted that the equations (25), (26), (27) discussed earlier are actually a simplified form of equations (28) for the zero angle of tilt.

The calculation of the final wind speed is realized on the basis of the calculation of the wind speed vector (29).

$$V_w = \sqrt{V_{wx}^2 + V_{wy}^2 + V_{wz}^2} \quad (29)$$

### 4 Results of simulation tests

In order to carry out algorithm tests and subsequent simulations and error tests, a mathematical model of the aircraft was necessary. It is available thanks to the *Matlab/Simulink* program plug-in called *Aerosim Blockset* [27], [28].

All the equations of motion mentioned above have been implemented in the model shown in Figure 3. Because the wind affects the flight behavior of the aircraft, it was required to create an external input for implementation in accordance with the algorithm specifications.

In addition, an additional component was introduced to the model to map the influence of wind. The model also includes control feedback loops, such as: automatic pilot with inclination or tilt function, inclination and deviation dampers, and servo models. Thanks to the above functions, it was possible to create several different flight paths to implement different environments and scenarios for testing the wind prediction algorithm [29].

#### 4.1 UAV model used in computer simulations

This subsection describes the components of the unmanned aerial vehicle used, on which a developed wind estimation algorithm was introduced through changes in the software. The parameters shown in the table below (Table 1) were implemented in the UAV model in *Matlab/Simulink* based on the mathematical analysis.

Table 1 Technical data of the UAV model

Technical data of the UAV	
Wingspan [mm]	1400
Fuselage length [mm]	980
Surface of the wings [dm <sup>3</sup> ]	38
Mass ready for flight [g]	1300
The drive battery Li-Pol 3S [mAh]	2200
Material	EPP foam

#### 4.2 Computer simulation

This section describes the results of a computer simulation study of the unmanned aerial vehicle model presented above to determine the effectiveness of the developed wind estimation algorithm [31-34]. In turn, the correctness of the wind prediction algorithm was tested using a

simplified realistic aircraft model in the *Matlab/Simulink* platform. The basics of this model are taken from the sample models from the *AeroSim Blockset* plug-in for the listed software.

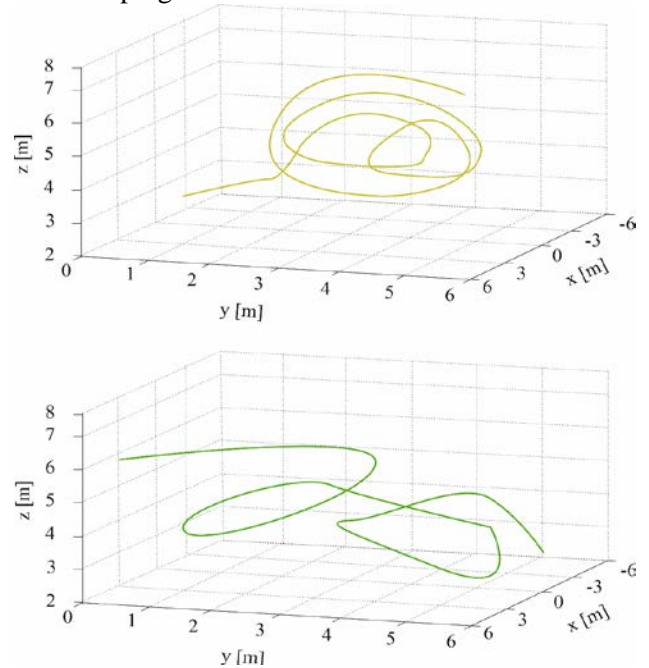


Fig. 3 Flight paths from computer simulation  
The simplified realistic model has been extended to implement an external wind and several basic automatic pilots. Several different flight paths were tested, and two examples shown in Figure 3.

The aircraft is exposed to wind at various speeds when flying along these paths. An example of these given wind speeds is given in Figure 4. Calculated speeds using the wind speed algorithm, were also presented on it.

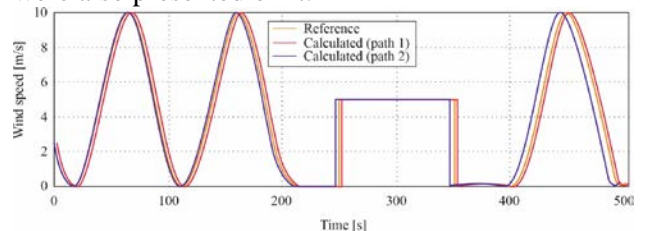


Fig. 4 Comparison of actual and estimated wind speed values

Based on the results obtained, it can easily be seen that the algorithm works correctly for simulation of a random flight path, giving accurate and correct calculation results (Figs. 5-8).

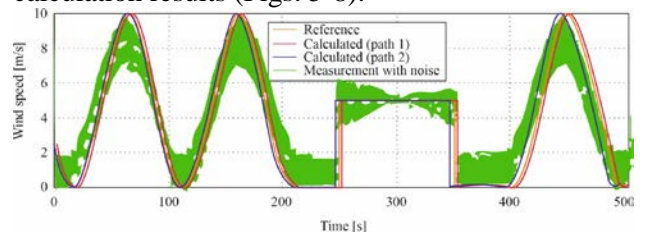


Fig. 5 Comparison of actual and estimated wind speed values for measurements with added noise

However, in real conditions it is almost impossible to achieve zero measurement error without the influence of external sensor noise, so additional white noise has been added to the measured values. It is noticeable that when UAV flies (moves) at an angle  $90^\circ$  from the wind direction, the error in estimating wind speed is almost zero (Fig. 5, at time:  $t = 75s$ ,  $t = 205s$  and  $t = 325s$ ).

It should be noted that in the graphs and analyzes presented above, only white noise of the size measuring sensor was assumed. Another dangerous phenomenon is the general deviation or drift of the values measured by the sensor. This type of error may result in unexpected system behavior. The next figure (Fig. 6) shows some deviation errors in the measurement of the attack angles.

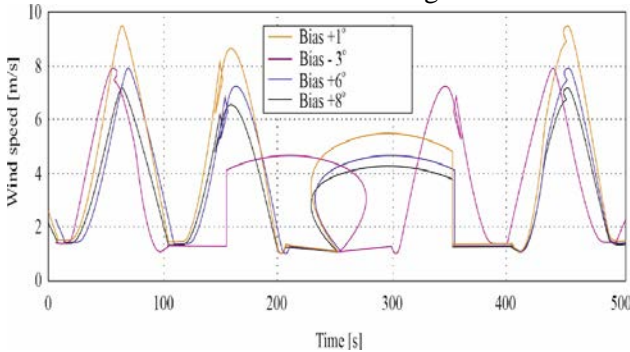


Fig. 6 Comparison of actual and estimated wind speed values with the calculated values with different values of the angle of attack measurement error

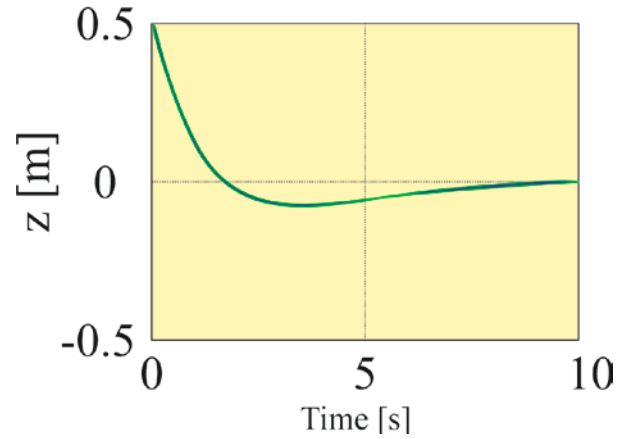
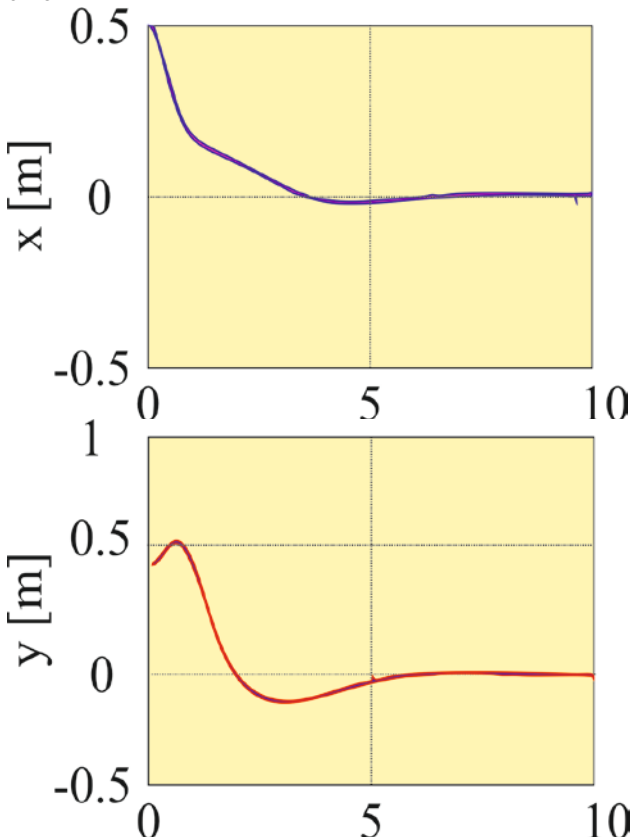


Fig. 7 The process of flight control during strong winds at 10 m/s

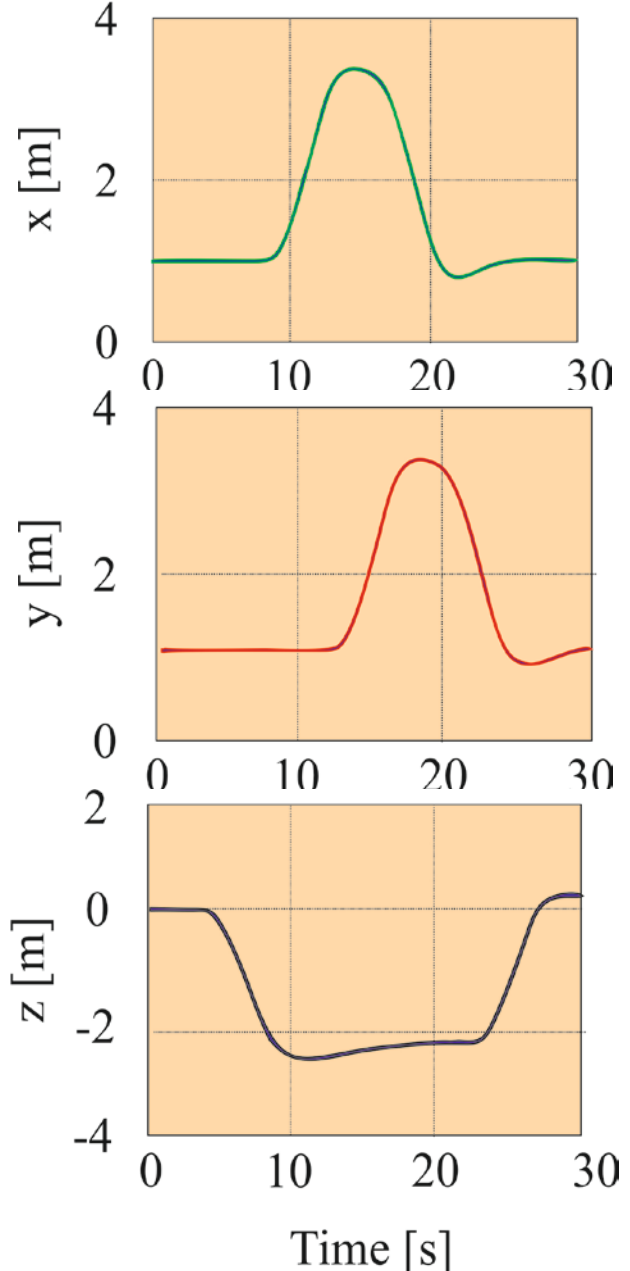


Fig. 8 The process of flight control during strong winds at 30 m/s

It is clear that different deviations have different effects on the final calculation of the wind speed value. For example, if all measured angle of attack values are greater by  $1^\circ$  than their actual value, the calculated wind speed is almost equal to or close to the real wind speed.

On the other hand, if the measured values of the angle of attack are greater than the real ones by  $3^\circ$ , in most cases the calculated wind speed differs significantly from its actual value.

## 5 Conclusions

This section summarizes the scope of work performed and its effects. The wind estimation algorithm has been developed and tested in several realistic simulations in Section 4.2.

Based on the output, it can be clearly stated that the calculations are carried out correctly and the results obtained are in accordance with the actual values of the measured parameters. An important aspect is that during the simulation there were variable wind conditions, which is a key element with which the algorithm works.

In addition, measurement errors were analyzed and their effect and impact on other measured values as well as the final results of flight parameters calculations were assessed.

Based on several of the aforementioned and discussed error analyzes and simulation methods, it was noticed that it would be advisable to develop and implement some type of advanced filter, e.g. *Kalman's*. This type of solution would ensure stable operation and resistance to measurement errors.

The developed algorithm was then saved in the C programming language and implemented into the flight controller system software. For testing the algorithm in a real environment, unmanned aircraft of the *Micro FunCub* class was used, with technical parameters given in Table 1.

During the flights, he carried out the instructions correctly, hence the conclusion on the proper functioning of the implemented software, however, exact calculations are not known due to the inability to save them.

In summary, the wind estimation algorithm used to support the flight control system of an unmanned micro-class aircraft has met the set requirements and can improve the operation of existing software.

In addition, this algorithm can also be used to compare data from the real environment with the values obtained during simulation using mathematical models in a virtual environment.

## References:

- [1] E. Nice, Design of a Four Rotor Hovering Vehicle, *Ph.D. dissertation, Cornell University*, 2004.
- [2] J. Tisdale, Z. Kim, and J. Hedrick, Autonomous UAV path planning and estimation, *IEEE Robotics Automation Magazine*, Vol. 16, No. 2, 2009, pp. 35-42.
- [3] E. Yanmaz, Robert Kuschnig On Path Planning Strategies for Networked Unmanned Aerial Vehicles, *IEEE INFOCOM*, 2011, pp. 212-216.
- [4] D.J. Balkcom, and M.T. Mason, Time optimal trajectories for bounded velocity differential drive vehicles, *International Journal of Robotics Research*, March 2002, pp.199-218.
- [5] L. Setlak and R. Kowalik, Studies of 4-rotor unmanned aerial vehicle UAV in the field of control system, 22nd International Conference on Circuits, Systems, Communications and Computers (CSCC 2018), *MATEC Web of Conferences*, Vol. 210, pp. 1-9, 2018.
- [6] N. Michael, D. Melinger, Q. Lindsey, and V. Kumar, The GRASP Multiple Micro UAV Testbed, *Robotics & Automation Magazine, IEEE*, 2010, pp. 56-65.
- [7] Nemati, and M. Kumar, Modeling and control of a single axis tilting quadcopter, In *American Control Conference (ACC)*, 2014, pp. 3077-3082.
- [8] Randal W. Beard, and Timothy W. McLain, Small unmanned aircraft: Theory and practice, *Princeton University Press*, 2012.
- [9] John H. Blakelock, Automatic Control of Aircraft and Missiles, *John Wiley & Sons*, 1991.
- [10] L. Setlak and R. Kowalik, MEMS Electro-mechanical Microsystem as a Support System for the Position Determining Process with the Use of the Inertial Navigation System INS and Kalman Filter, *WSEAS Transactions on Applied and Theoretical Mechanics*, Vol. 14, 2019, pp. 105-117.
- [11] H. J. Sussmann, and G. Tang, Shortest paths for the Reeds-Shepp car: A worked out example of the use of geometric techniques in nonlinear optimal control, *Technical Report SYNCON 91-10*, Department of Mathematics, Rutgers University, 1991.
- [12] Nemati, and M. Kumar, Non-Linear Control of Tilting Quadcopter Using Feedback Linearization Based Motion Control, *Dynamic System and Control Conference (DSCC)*, 2014.
- [13] Brian L. Stevens, Frank L. Lewis, and Eric N. Johnson, Aircraft Control and Simulation:

Dynamics, Controls Design, and Autonomous Systems, *John Wiley & Sons*, 2015.

- [14] Davide Del Cont Bernard, Fabio Riccardi, Mattia Giurato, and Marco Lovera. A dynamic analysis of ground eject for a quadrotor platform, *20th IFAC World Congress*, Toulouse, France, 2017.
- [15] L. Setlak, R. Kowalik, S. Bodzon, The Study of Air Flows for an Electric Motor with a Nozzle for an Unmanned Flying Platform, *WSEAS Transactions on Fluid Mechanics*, Vol. 14, 2019, pp. 21-35.
- [16] P.B. Sujit, Srikanth Saripalli, and Joao Borges Sousa, Unmanned aerial vehicle path following: A survey and analysis of algorithms for fixed-wing unmanned aerial vehicles, *IEEE Control Systems*, 34(1): 2014, pp. 42-59.
- [17] Katsuhiko Ogata and Yanjuan Yang, Modern Control Engineering, *Prentice-Hall Englewood Cliffs*, NJ, 1970.
- [18] Eugene Lavretsky, and Kevin A. Wise, Robust adaptive control, In *Robust and Adaptive Control*, Springer, 2013. pp. 317-353.
- [19] Hassan K. Khalil, Nonlinear systems, *Prentice-Hall*, New Jersey, 2002.
- [20] Derek R. Nelson, D. Blake Barber, Timothy W. McLain, and Randal W. Beard, Vector field path following for miniature air vehicles, *IEEE Transactions on Robotics*, 23(3): 2007, pp. 519-529.
- [21] Sanghyuk Park, John Deyst, and Jonathan P. How, A new nonlinear guidance logic for trajectory tracking, In *AIAA guidance, navigation, and control conference and exhibition*, 2004, pp. 16-19.
- [22] L.F. Faleiro and A.A. Lambregts, Analysis and tuning of a total energy control system control law using eigen structure assignment, *Aerospace Science and Technology*, 3(3): 1999, pp. 127-140.
- [23] L. Setlak, R. Kowalik, Stability Evaluation of the Flight Trajectory of Unmanned Aerial Vehicle in the Presence of Strong Wind, *WSEAS Transactions on Systems and Control*, Vol. 14, 2019, pp. 51-56.
- [24] Petros A. Ioannou, and Jing Sun, Robust adaptive control, Volume 1. *PTR Prentice-Hall Upper Saddle River*, NJ, 1996.
- [25] H. Chitsaz, S.M. LaValle, D.J. Balkcom, and M.T. Mason, An explicit characterization of minimum wheel-rotation paths for differential drives, In *Proceedings 12th IEEE International Conference on Methods and Models in Automation and Robotics*, 2006.
- [26] J.D. Boissonnat, A. Cerezo, and J. Leblond, Shortest paths of bounded curvature in the plane, *J. Intelligent and Robotic Systems*, 1994, pp. 5-20.
- [27] S.L. Waslander, J.S. Jang, C.J. Tomlin, Multi-Agent X4-Flyer Testbed Control Design: Integral Sliding Mode vs. Reinforcement Learning, *IEEE Conference on Intelligent Robots and Systems*, 2009.
- [28] N. Guenard, T. Hamel, V. Moreau, and S.A. France, Dynamic Modeling and Intuitive Control Strategy for an X4-flyer, in *ICCA'05 International Conference on Control and Automation*, 2005, pp. 1-6.
- [29] Blum, P. Raghavan, and B. Schieber, Navigating in unfamiliar terrain, In *STOC*, 1991, pp. 494-504.
- [30] J.Y. Potvin, A Review of Bio-inspired Algorithms for Vehicle Routing, *Problem*, Vol. 161, 2009, pp. 1-34.
- [31] L. Setlak, R. Kowalik, Analysis, Mathematical Model and Simulation Tests of the Unmanned Aerial Vehicle Control System, *WSEAS Transactions on Systems and Control* Vol. 14, pp. 51-56, 2019.
- [32] J.A. Reeds and L.A. Shepp, Optimal paths for a car that goes both forwards and backwards, *Pacific J. Math.*, 1990, pp. 367-393.
- [33] L.E. Dubins, On curves of minimal length with a constraint on average curvature, and with prescribed initial and terminal positions and tangents, *American Journal of Mathematics*, Vol. 79, 1957, pp. 497-516.
- [34] S. Poduri, and G.S. Sukhatme, Constrained coverage for mobile sensor networks, in *Proceedings IEEE International Conference Robotics and Automation*, 2004, pp. 165-172.